


Downregulation of miR-199a-3p in Hepatocellular Carcinoma and Its Relevant Molecular Mechanism via GEO, TCGA Database and In Silico Analyses

Technology in Cancer Research & Treatment
Volume 19: 1-17
© The Author(s) 2020
Article reuse guidelines:
sagepub.com/journals-permissions
DOI: 10.1177/1533033820979670
journals.sagepub.com/home/tct


An-gui Liu, BMed¹, Yu-yan Pang, MD², Gang Chen, MD², Hua-Yu Wu, MD³, Rong-Quan He, MD¹, Yi-wu Dang, MD², Zhi-guang Huang, MD², Rui Zhang, MD², Jie Ma, MD^{1,2} , and Li-hua Yang, MD¹

Abstract

Existing reports have demonstrated that miR-199a-3p plays a role as a tumor suppressor in a variety of human cancers. This study aims to further validate the expression of miR-199a-3p in HCC and to explore its underlying mechanisms by using multiple data sets. Chip data or sequencing data and quantitative reverse transcription polymerase chain reaction (qRT-PCR) were integrated to assess the expression of miR-199a-3p in HCC. The potential targets and transcription factor regulatory network of miR-199a-3p in HCC were determined and possible biological mechanism of miR-199a-3p was analyzed with bioinformatics methods. In the results, miR-199a-3p expression was significantly lower in HCC tissues compared to normal tissues according to chip data or sequencing data and qRT-PCR. Moreover, 455 targets of miR-199a-3p were confirmed, and these genes were involved in the PI3K-Akt signaling pathway, pathways in cancer, and focal adhesions. LAMA4 was considered a key target of miR-199a-3p. In CMTCN, 11 co-regulatory pairs, 3 TF-FFLs, and 2 composite-FFLs were constructed. In conclusion, miR-199a-3p was down regulated in HCC and LAMA4 may be a potential target of miR-199a-3p in HCC.

Keywords

hepatocellular carcinoma, miR-199a-3p, Gene Expression Omnibus, qRT-PCR

Abbreviations

HCC, Hepatocellular Carcinoma; qRT-PCR, Quantitative Reverse Transcription PCR; miRNA, microRNAs; SRA, Sequence Read Archive; GEO, Gene Expression Omnibus; TCGA, The Cancer Genome Atlas; SMD, standard mean difference; ROC, receiver operating curve; sROC, summarized ROC; DEGs, differentially expressed genes; PPI, protein-protein interaction; TF, transcription factor; FFLs, feed-forward loops; GO, Gene ontology; KEGG, Kyoto Encyclopedia of Genes and Genomes

Received: November 16, 2019; Revised: October 13, 2020; Accepted: November 03, 2020.

Introduction

Hepatocellular carcinoma (HCC) is a major malignant cancer and one of the leading causes of malignancy-associated mortality worldwide.¹ The development of treatment approaches to HCC have improved with the help of large-scale, cancer-related research.^{2,3} Nevertheless, HCC evolves rapidly, which results in low survival times.^{4,5} Thus, it is urgent to continuously explore the biological mechanisms of HCC in tumorigenesis or progression, and identifying the potential biomarkers or regulators for HCC treatment is imperative.

MicroRNAs (miRNAs) are small, single-stranded, non-coding RNAs of 18 to 25 nucleotides in length that are

¹ Department of Oncology, The First Affiliated Hospital of Guangxi Medical University, Nanning, Guangxi Zhuang Autonomous Region, People's Republic of China

² Department of Pathology, The First Affiliated Hospital of Guangxi Medical University, Nanning, Guangxi Zhuang Autonomous Region, People's Republic of China

³ Departments of Cell Biology and Genetics, School of Pre-clinical Medicine, Guangxi Medical University, Nanning, Guangxi, People's Republic of China

Corresponding Authors:

Jie Ma and Li-hua Yang, Department of Oncology, The First Affiliated Hospital of Guangxi Medical University, Nanning, Guangxi Zhuang Autonomous Region 530021, People's Republic of China.

Emails: majie@gxmu.edu.cn; yanglihua@gxmu.edu.cn



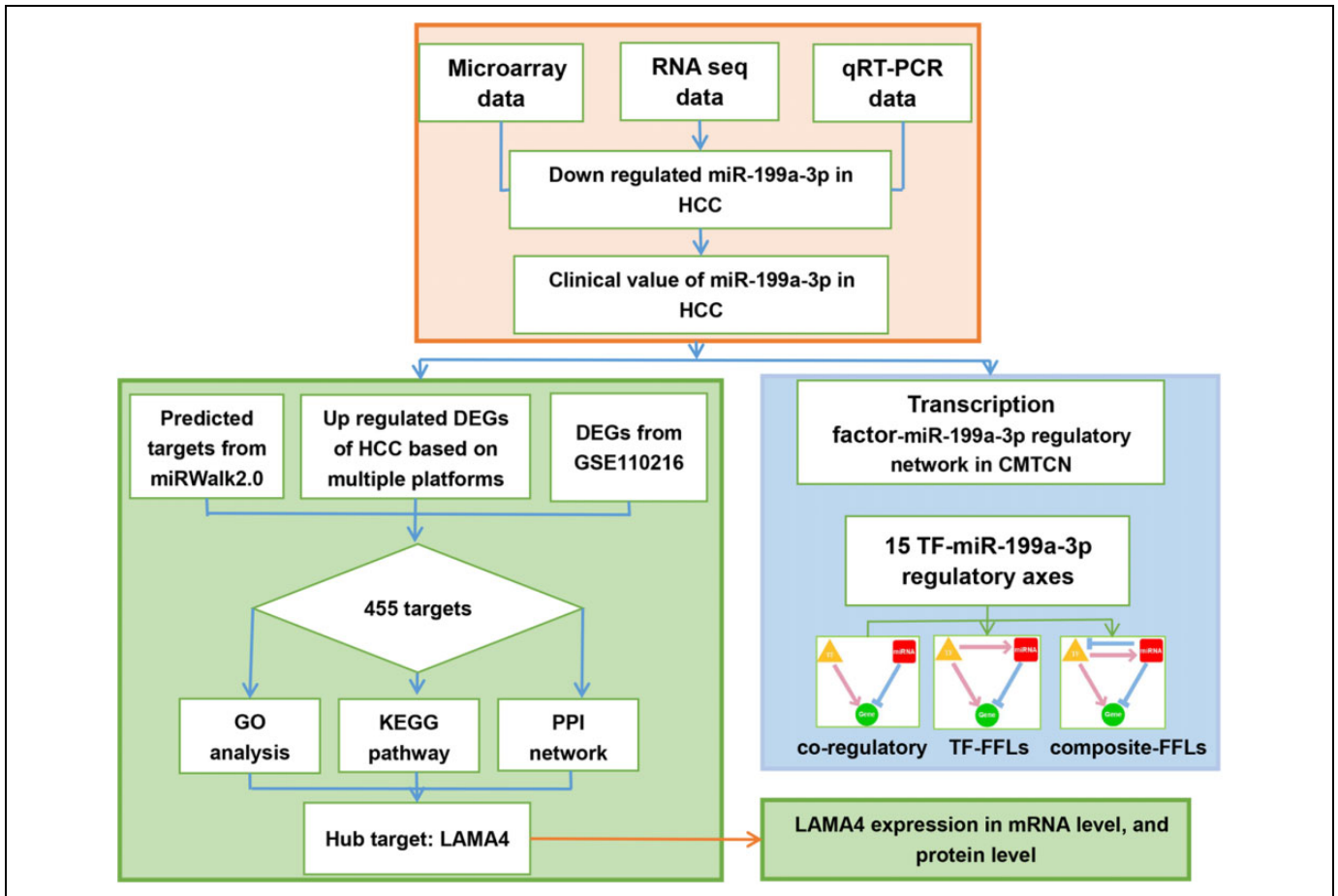


Figure 1. The flow chart represents the main design of this study. The study is divided into 3 parts, including the evaluation of miR-199a-3p expression in HCC by integrating multiple data sets, the identification of the potential targets of miR-199a-3p in HCC, and the construction of the transcription factor and miR-199a-3p regulatory network.

transcribed by DNA⁶ (31557962) MicroRNAs can combine to target a gene's 3'UTR region and function to control the expression of the target gene in post-transcription. According to the degree of sequence complementarity, miRNAs could cause the reduction of the target gene or inhibit the translation of mRNA, thus interfering protein synthesis.^{7,8} Published studies have shown that miRNA is an important regulator of functional gene expression and reveal a crucial function in the occurrence and evolution of diseases.^{9,10} Existing reports have documented that miRNAs may participate in the occurrence and evolution of multiple cancers and may offer a new strategy for cancer screening, diagnosis, prognosis, and treatment.^{11,12} In HCC, numerous miRNAs have been reported to be aberrantly expressed and the dysregulation of these miRNAs has been reported to exist potential clinical values.¹³⁻¹⁵

One miRNA, miR-199a-3p, has been reported to function in several tumors, such as esophageal cancer,¹⁶ prostate cancers,¹⁷ and papillary thyroid cancer.¹⁸ The dysregulation of miR-199a-3p in HCC in particular has aroused our concern. It has been reported that miR-199a-3p can function as a new marker for the diagnosis and treatment of HCC patients.^{19,20} Moreover, miR-199a-3p inhibits HCC growth through modulating MTOR

and PAK4 pathway.²¹ In addition, miR-199a-3p was found to inhibit the tumorigenesis, growth, migration, invasion, and angiogenesis of HCC by targeting multiple targets, such as PUMA or ZHX1,²² VEGFA, VEGFR1, VEGFR2, HGF, MMP2,²³ YAP1, Jagged1, Notch signaling,²⁴ and CD151.²⁵ Although previous studies have tried to verify the expression of miR-199a-3p in HCC, small sample data may reduce the reliability of the results.

In the current study, chip data or sequencing data and quantitative reverse transcription polymerase chain reaction (qRT-PCR) were integrated to assess the expression of miR-199a-3p in HCC. We also screened the potential targets and transcription factor regulatory network of miR-199a-3p in HCC and analyzed the possible biological mechanism of miR-199a-3p with bioinformatics methods (Figure 1).

Materials and Methods

HCC Tissue Sample Collection

In this study, 26 pairs of HCC tissue samples and adjacent tissue samples were collected from 26 patients diagnosed and undergoing surgery in our unit from March 2010 to December

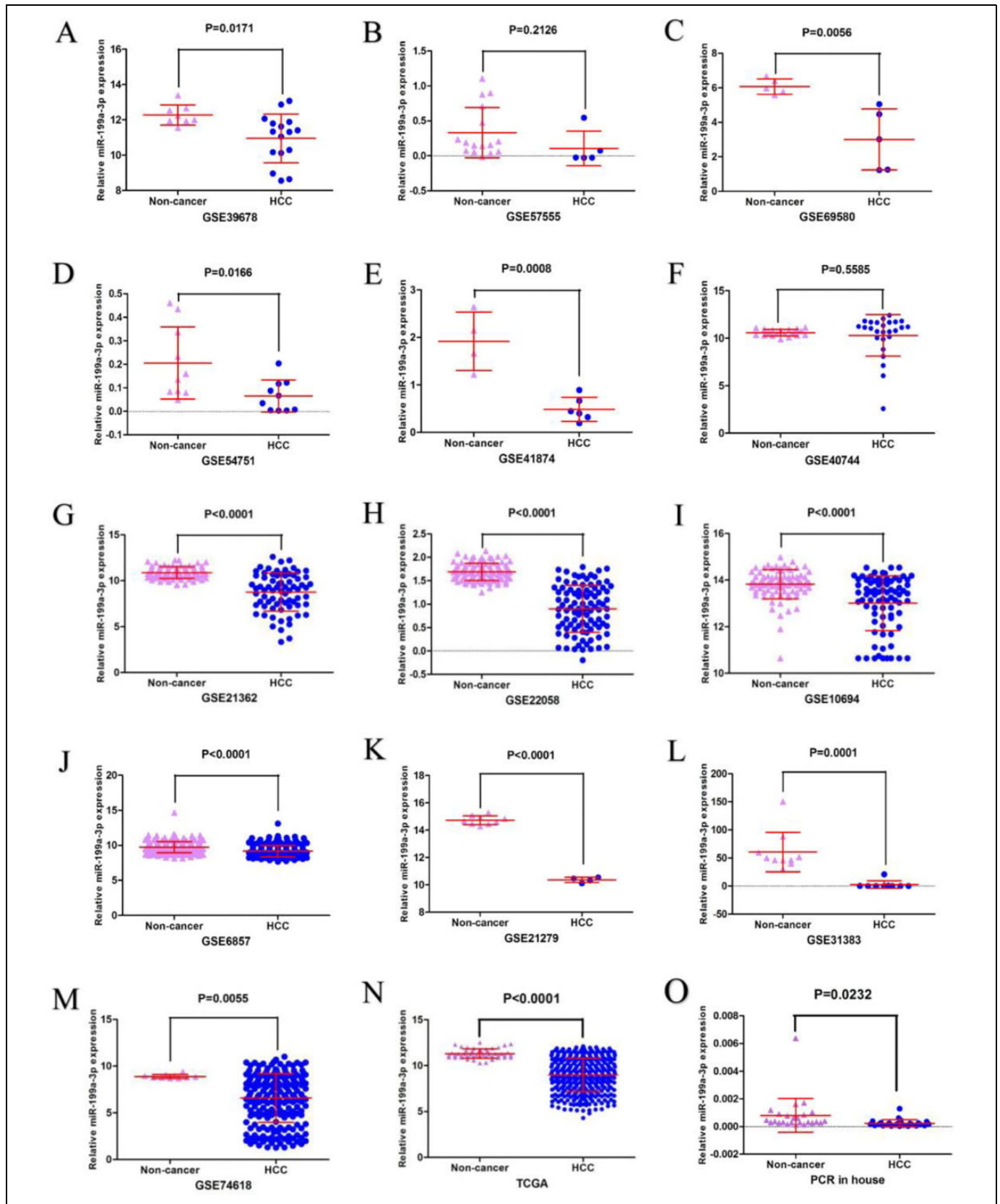


Figure 2. The evaluation of miR-199a-3p expression in HCC based on HCC chip data and sequencing data and qRT-PCR. A: GSE39678, B: GSE57555, C: GSE69580, D: GSE54751, E: GSE41874, F: GSE40744, G: GSE21362, H: GSE22058, I: GSE10694, J: GSE6857, K: GSE21279, L: GSE31383, M: GSE74618, N: TCGA, O: qRT-PCR.

Table 1. The Evaluation of miR-199a-3p Expression in HCC Based on HCC Chip Data and Sequencing Data and qRT-PCR.

Data sets	Year	HCC group			Normal group			T	P-value
		Number	Mean	SD	Number	Mean	SD		
GSE39678	2012	16	10.9494	1.38375	8	12.2753	0.57091	3.311	0.003
GSE57555	2015	5	0.108	0.24777	16	0.3326	0.36055	1.29	0.213
GSE69580	2015	5	3.0052	1.77066	5	6.0702	0.44323	3.755	0.016
GSE54751	2014	10	0.0646	0.06766	10	0.2047	0.15345	2.641	0.021
GSE41874	2013	6	0.4867	0.25275	4	1.9163	0.61419	5.2	0.001
GSE40744	2013	26	10.2954	2.19382	19	10.5958	0.34837	0.686	0.498
GSE21362	2011	73	8.7558	2.06615	73	10.8862	0.62893	8.428	P < 0.001
GSE22058	2010	96	0.8999	0.50202	96	1.6875	0.18284	14.444	P < 0.001
GSE10694	2008	78	13.0086	1.17368	88	13.8224	0.62837	5.469	P < 0.001
GSE6857	2008	241	8.9864	1.5437	241	9.7475	0.79746	6.801	P < 0.001
GSE21279	2010	4	10.3619	0.18905	9	14.7251	0.32472	24.697	P < 0.001
GSE31383	2012	9	2.5256	6.89372	10	60.6199	35.00255	5.139	P < 0.001
GSE74618	2016	223	6.5807	2.6072	10	8.894	0.21716	12.33	P < 0.001
TCGA	2018	372	8.9839	1.82456	48	11.3066	0.51513	19.304	P < 0.001
PCR in house	—	26	0.0002	0.00026	26	0.0008	0.00122	-2.342	0.027

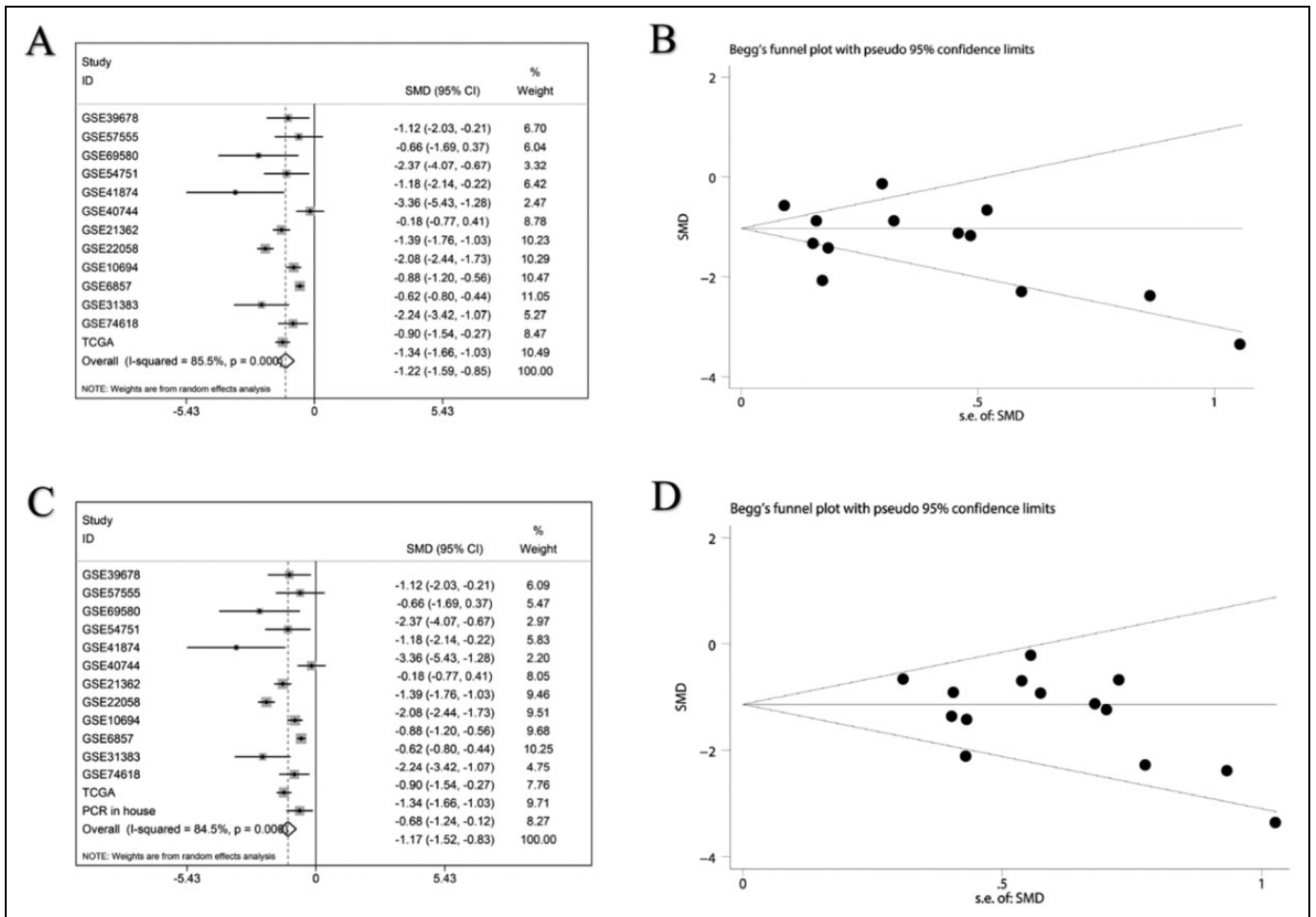


Figure 3. The evaluation of miR-199a-3p expression in HCC with meta-analysis based on HCC chip data and sequencing data and qRT-PCR. A: the forest plot based on HCC chip data and sequencing data; B: the funnel plot based on HCC chip data and sequencing data; C: the forest plot after adding qRT-PCR data; D: the forest plot after adding qRT-PCR data.

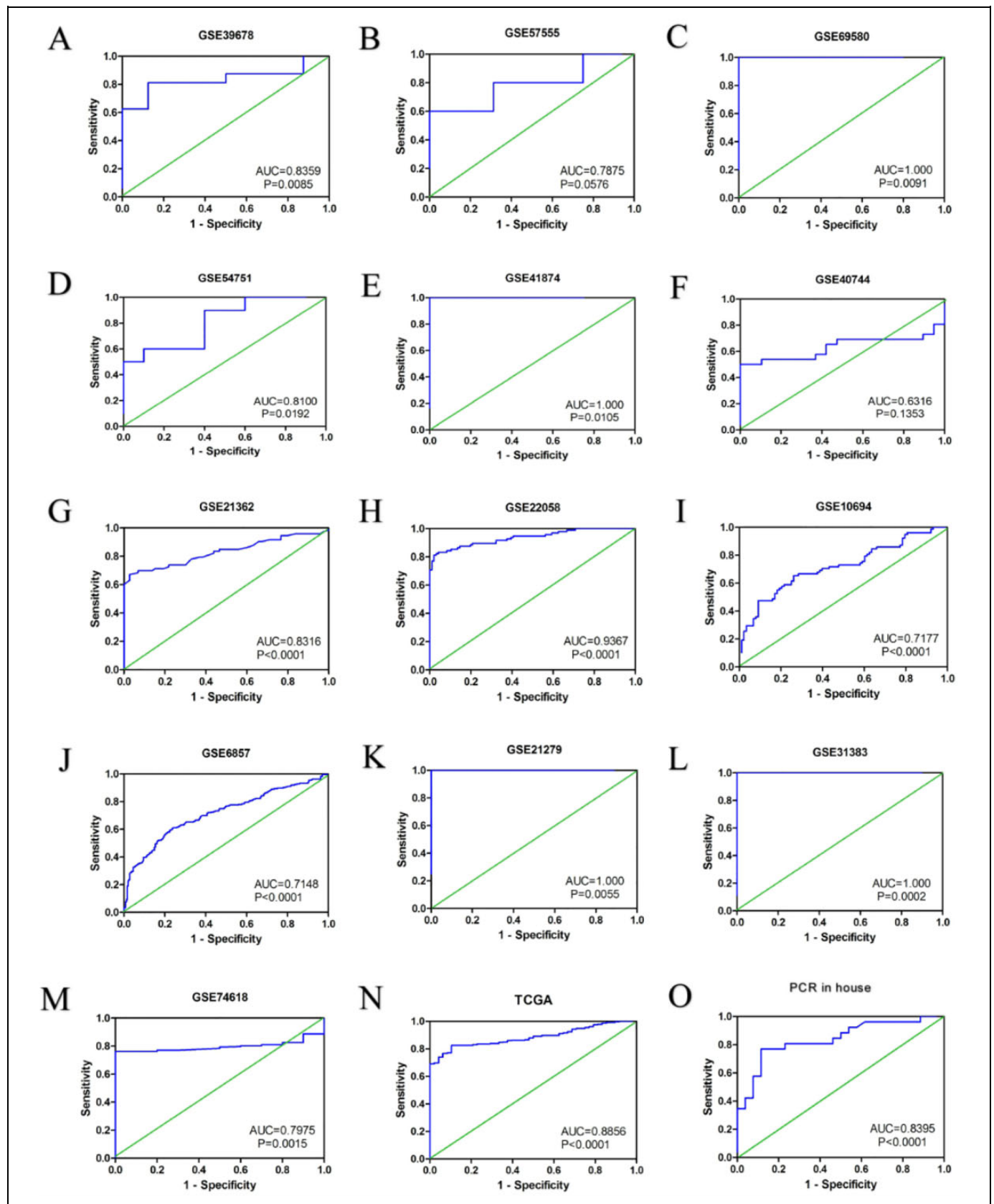


Figure 4. The receiver operating curve (ROC) based on HCC chip data and sequencing data and qRT-PCR data. A: GSE39678, B: GSE57555, C: GSE69580, D: GSE54751, E: GSE41874, F: GSE40744, G: GSE21362, H: GSE22058, I: GSE10694, J: GSE6857, K: GSE21279, L: GSE31383, M: GSE74618, N: TCGA, O: qRT-PCR.

Table 2. The Potential of miR-199a-3p in Differentiating HCC Tissues From Normal Tissues.

Data sets	Sensitivity	Specificity	TP	FP	FN	TN
GSE39678	0.8125	0.875	13	1	3	7
GSE57555	0.6	1	3	0	2	16
GSE69580	1	1	5	0	0	5
GSE54751	0.6	0.9	6	1	4	9
GSE41874	1	1	6	0	0	4
GSE40744	0.5	1	13	0	13	19
GSE21362	0.6712	0.9726	49	2	24	71
GSE22058	0.8125	0.9792	78	2	18	94
GSE10694	0.4744	0.9091	37	8	41	80
GSE6857	0.6102	0.7593	147	58	94	183
GSE21279	1	1	4	0	0	9
GSE31383	1	1	9	0	0	10
GSE74618	0.7623	1	170	0	53	10
TCGA	0.8958	0.8253	333	9	39	39
PCR in house	0.7692	0.8846	20	3	6	23

TP: true positive; FP: false positive; FN: false negative; TN: true negative.

2011. Some of the clinical or pathological information of these patients was also collected, including age, gender, clinical stage, tumor size, and vascular invasion.

RT-qPCR

Total RNA was detected in FFPE sections using the miRNeasy FFPE Kit, and the concentration of RNA was identified with NanoDrop 2000. The real-time quantitative PCR was conducted by utilizing the Applied Biosystems 7900HT Fast Real-Time PCR System, and the miRNA expression was detected based on the operation guide of the merchant. The formula $2^{-\Delta Ct}$ was exploited to calculate the expression data of miR-199a-3p.

Data Collection

The data sets of miR-199a-3p expression in HCC tissues and healthy tissues were screened in the Sequence Read Archive

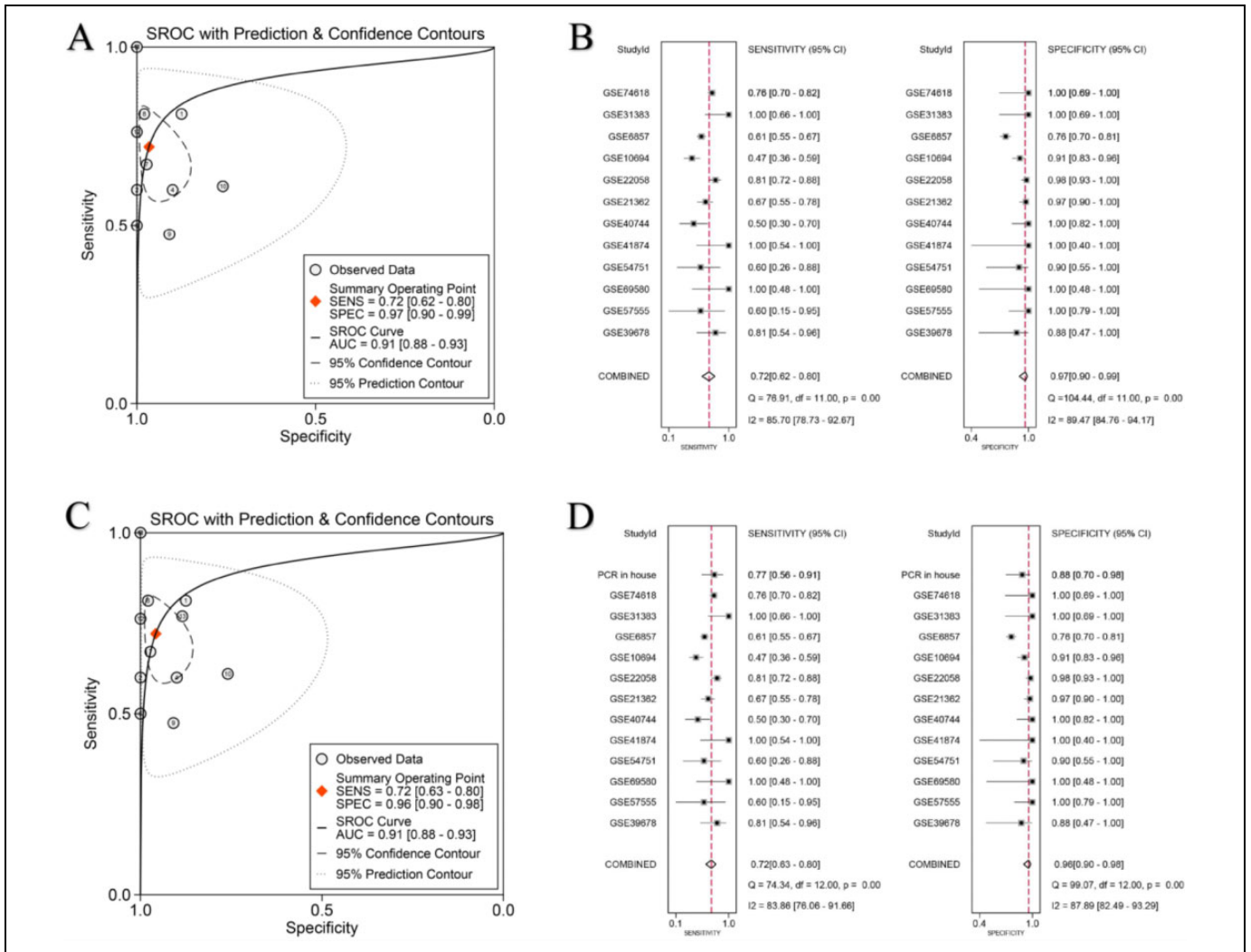


Figure 5. The sROC based on HCC chip data and sequencing data and qRT-PCR. A: the sROC based on HCC chip data and sequencing data; B: the corresponding sensitivity and specificity; C: the sROC after adding qRT-PCR data; D: the corresponding sensitivity and specificity after adding qRT-PCR data.

(SRA), the Gene Expression Omnibus (GEO), the ArrayExpress Archive of Functional Genomics Data, The Cancer Genome Atlas (TCGA) database, and OncoPrint with the following search strategy: (miR OR miRNA OR microRNA) AND (cancer OR tumor OR carcinoma) AND (hepatocellular OR liver OR hepatic OR HCC). The screening strategy was as follows: First, each data set should contain human HCC tissue samples and normal tissue samples. Second, liver cirrhotic tissue samples were not included in our non-tumor group. Third, the miRNA expression data could be obtained from all included data sets. The miR-199a-3p expression data for each data set were collected and divided into HCC groups and normal groups. The HCC sequencing data of the TCGA database were downloaded from UCSC Xena (<https://xena.ucsc.edu/>), which included the sequencing data for 371 HCC and 48 normal tissues. The data were processed as microarray data. The HCC-related clinical parameters, including gender, grade, age, TNM stage, and survival data, were also extracted from the TCGA database.

Differentially Expressed Analysis

HCC mRNA-related chip data or sequencing data were searched in the GEO database using the keywords (cancer OR tumor OR carcinoma) AND (hepatocellular OR liver OR hepatic OR HCC). The included data set must meet the following conditions: First, the mRNA expression profiles in HCC tissues or normal tissues could be achieved. Second, more than 3 tumors and controls were included in the study. The microarray data of included data sets were produced by multiple platforms and normalized by using the RMA algorithm provided by the Linear Models for Microarray Data (Limma) package (<http://bioconductor.org/packages/limma/>). The sva package of R software was exploited to remove the batch effect. Finally, the Limma package of R was used to perform the differentially expressed analysis, and the differentially expressed gene of each platform was calculated. P-value < 0.05 and |fold change(FC)| > 1 were regarded as significant.

Potential Target Genes of miR-199a-3p

GSE110216 was a microarray that included miR-199a-3p overexpressed and untreated HCC cell lines. GEO2 R was used to carry out a differentially expressed analysis between miR-199a-3p overexpressed and untreated HCC cell lines, and $\log_{2}FC < -1$ was regarded as significant. MiRWalk2.0 was used to predict the targets of miR-199a-3p. MiRWalk 2.0 is a collection of predictive tools that includes 12 online predicted tools. Genes predicted by more than 3 tools were accepted. The overlapped genes of upregulated differentially expressed genes (DEGs) of HCC, downregulated genes from differentially expressed analysis of overexpressed and untreated HCC cell lines, and predicted targets of miR-199a-3p were considered as possible targets of miR-199a-3p in HCC.

GO and KEGG Analysis

Gene ontology and KEGG analysis were carried out in the Database for Annotation, Visualization and Integrated Discovery (DAVID) (<https://david.ncifcrf.gov/>) to decipher the functions of target genes. The STRING database (<https://string-db.org/>) was used to perform protein-protein interaction (PPI) analysis. Based on the results of enrichment analysis and PPI analysis, the hub target genes of miR-199a-3p were confirmed.

Validating the Expression Level and Clinical Role of Hub Genes

The mRNA expression of hub genes were assessed via a meta analysis by integrating the GEO microarray data or TCGA RNA-seq data, while the protein expression of hub genes was assessed based on the immunohistochemistry data of The Human Protein Atlas (<https://www.proteinatlas.org/>). In addition, a summary receiver operating characteristic (sROC) curve was produced to provide a further assessment of the potential of hub genes to differentiate HCC tissues from normal tissues. The prognosis-related GEO data and TCGA RNA-seq data were collected, and a prognosis meta-analysis was performed for the hub genes.

Construction of Transcription Factor Network

CMTCN (<http://www.cbportal.org/CMTCN/>) is an online tool for exploring cancer-specific miRNAs and transcription factor regulatory networks. Four types of miRNAs and transcription factor regulatory models were provided in CMTCN, included co-regulatory pairs, TF-FFLs, miRNA-FFLs, and composite-FFLs. We constructed miR-199a-3p-related transcription factor regulatory networks in this web.

Statistical Analysis

The software packages Stata 12 and SPSS 19 were used for our statistical analysis. First, RT-PCR, chip data, or sequencing data was calculated with an independent sample t-test or a paired sample t-test in SPSS 19 to assess the expression of miR-199a-3p in HCC and normal tissue samples. The relationship of miR-199a-3p expression and clinicopathological parameters were assessed by t-test or variance analysis. Second, Stata 12 was used to integrate the results of the t-tests based on RT-PCR, chip data, or sequencing data through a meta-analysis. The fixed effects model was used for the initially and the random effects model was used when $I^2 > 50\%$, which identified the existence of heterogeneity. Third, ROC curves based on included data were drawn to assess the reliability of miR-199a-3p in distinguishing HCC and normal tissue samples. An sROC was also performed via a meta-analysis.

Table 3. The Relationship Between miR-199a-3p Expression and Clinicopathological Features Based on TCGA Data.

Clinicopathological Feature		Number	miR-199a-3p expression (2-ΔCq)		T	P-value
			Mean ± SD			
Tissue	HCC	371	8.9839 ± 1.82456		19.304	0
	Non-tumor	48	11.3066 ± 0.51513			
Gender	Male	252	8.9605 ± 1.82871		0.278	0.781
	Female	119	9.0171 ± 1.82205			
Age	<60	171	9.1781 ± 1.85097		1.954	0.051
	≥60	200	8.8082 ± 1.78822			
Stage	I-II	258	8.9 ± 1.86501		-0.648	0.517
	III-IVB	90	9.0457 ± 1.75452			
Histologic grade	G1	55	9.0371 ± 1.69797		F = 1.134	0.335
	G2	174	9.0356 ± 1.91936			
	G3	125	8.9805 ± 1.7301			
	G4	13	8.076 ± 1.94426			
M stage	M0	268	8.9119 ± 1.84721		F = 0.654	0.52
	M1	4	9.2694 ± 1.74054			
	MX	99	9.1478 ± 1.7696			
N stage	N0	254	8.9094 ± 1.86353		F = 0.47	0.625
	N1	4	9.0417 ± 2.212			
	NX	112	9.1094 ± 1.71809			
T stage	T1-T2b	275	8.9328 ± 1.86228		F = 0.56	0.455
	T3-T4	94	9.096 ± 1.70862			

Results

MiR-199a-3p Expression in HCC Tissues

MiR-199a-3p expression was initially evaluated in HCC tissues and healthy tissues based on the GEO data sets. A total of 13 GEO data sets, which included both HCC tissues and healthy tissues, were collected in our study. Downregulated miR-199a-3p was observed in 11 data sets, whereas no significant differences were found in the other 2 GEO data sets (GSE57555 and GSE40744). Under-expressed miR-199a-3p was also found in 372 HCC tissues (8.9839 ± 1.82456) compared with 48 adjacent non-cancerous HCC tissues (11.3066 ± 0.51513 , $P < 0.001$) based on the TCGA sequencing data (Figure 2, Table 1). Significant downregulated miR-199a-3p was found in HCC tissues by integrating all the included GEO data sets and The Cancer Genome Atlas (TCGA) sequencing data (SMD = -1.22 ; 95% CI, -1.59 to -0.85 ; $P < 0.001$) with heterogeneity using the random effects model ($P < 0.001$, $I^2 = 85.5\%$) (Figure 3A-B). Moreover, downregulated miR-199a-3p was also found in our qRT-PCR based on the 26 pairs of clinical HCC tissues and normal tissues, and the corresponding SMD of the random effects model was -1.17 (-1.52 , -0.83) with $I^2 = 84.5\%$ (Figure 3C-D). MiR-199a-3p could be a valuable marker to distinguish HCC tissues from normal tissues with an area under the curve (AUC) of 1.00 based on HCC chip data (GSE69580, GSE41874, GSE31383). Additionally, the ROC based on the TCGA sequencing data and the qRT-PCR also indicated that miR-199a-3p has the potential to be a marker for distinguishing HCC from normal tissue samples, with the AUC being 0.8856 and 0.8395, respectively (Figure 4, Table 2). The sROC calculated based on HCC chip data and sequencing data was 0.91 (0.88, 0.93) with a pooled sensitivity and

Table 4. The Relationship Between miR-199a-3p Expression and Clinicopathological Features Based on qRT-PCR Data.

Clinicopathological Feature		Number	miR-199a-3p expression (2-ΔCq)		T	P-value
			Mean ± SD			
Tissue	HCC	26	0.0002 ± 0.00026		-2.342	0.027
	Non-tumor	26	0.0008 ± 0.00122			
Gender	Male	20	0.0002 ± 0.00029		0.769	0.449
	Female	6	0.0002 ± 0.00007			
Age	<50	11	0.0003 ± 0.00035		-0.59	0.561
	≥50	15	0.0002 ± 0.00017			
Stage	I-II	6	0.0002 ± 0.0001		-0.14	0.989
	III-IV	20	0.0002 ± 0.00029			
Metastasis	Yes	20	0.0002 ± 0.0001		-0.14	0.989
	No	6	0.0002 ± 0.00029			
Node	Single	11	0.0002 ± 0.00011		-0.872	0.392
	Multiple	15	0.0003 ± 0.00033			
Size	<5cm	7	0.0002 ± 0.00015		-0.258	0.799
	≥5cm	19	0.0002 ± 0.00029			
Vascular invasion	No	15	0.0002 ± 0.00016		0.066	0.948
	Yes	11	0.0002 ± 0.00036			

specificity of 0.72 (0.62, 0.80) and 0.97 (0.90, 0.99), respectively (Figure 5A-B). The corresponding sROC based on the HCC chip data, sequencing data, and qRT-PCR was 0.91 (0.88, 0.93) with a corresponding sensitivity and specificity of 0.72 (0.63, 0.80) and 0.96 (0.90, 0.98), respectively (Figure 5C-D). In addition, no significant differences were found in the other clinical features (Tables 3 and 4).

Identification of miR-199a-3p Targets

In total, 68 groups of HCC mRNA-related microarrays and RNA-seq data were screened. These data sets are divided into 8 platforms, and data from the same platform was merged and removed the batch effects. The differentially expressed analysis was performed based on each of these 8 platforms. A total of 3006 upregulated genes intersected by more than 3 platforms were accepted. P -value < 0.05 and $|\text{fold change (FC)}| > 2$ were regarded as significant. After differential expression analysis between miR-199a-3p overexpressed and untreated HCC cell lines based on GSE110216, a total of 6434 downregulated genes were obtained. Meanwhile, a total of 9600 targeted genes of miR-199a-3p were predicted in miRWalk 2.0. Finally, 3006 upregulated DEGs of HCC, 6434 downregulated genes from differentially expressed analysis of overexpressed and untreated HCC cell lines, and 9600 predicted targets of miR-199a-3p overlapped, and 455 overlapped genes were considered possible targets of miR-199a-3p in HCC (Figure 6A, Supplementary Figure 1).

Functional Analysis of the Targets of miR-199a-3p in HCC

First, the functional roles of 455 potential target genes in GO enrichment analysis were identified. The analysis indicated that numerous target genes were related to signal transduction, plasma membrane, and transmembrane receptor protein tyrosine kinase activity (Table 5, Figure 6B-D). The KEGG

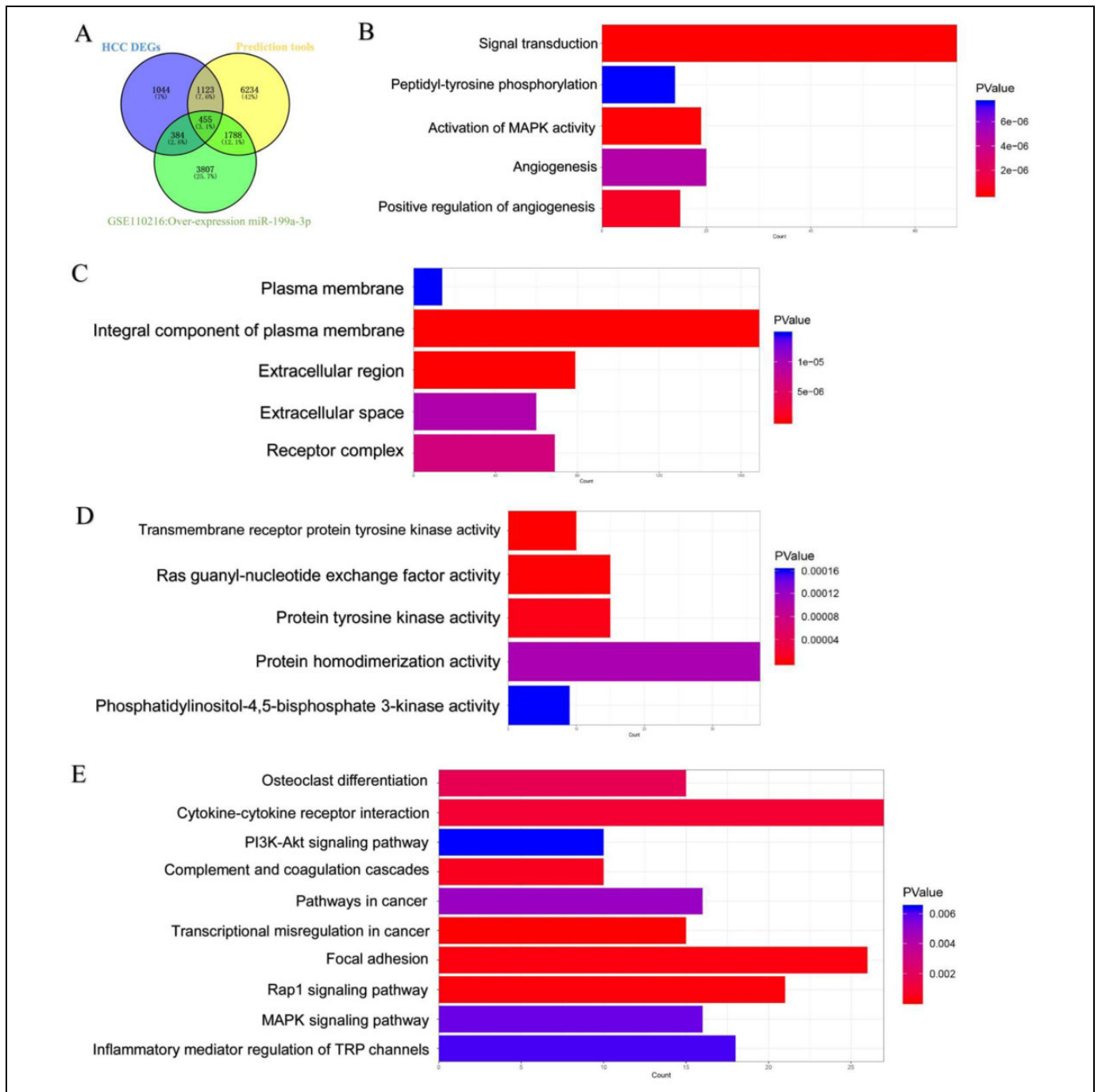


Figure 6. The enrichment analysis based on target genes of miR-199a-3p. A: the potential targets of miR-199a-3p in HCC; B: biological process; C: cell component; D: molecular function; E: KEGG pathways.

pathways revealed some important pathways, such as the PI3K-Akt signaling pathway, pathways in cancer, and focal adhesion (Table 5, Figure 6E).

The PPI Network and Verification of Hub Target Genes

The genes that were enriched in the PI3K-Akt signaling pathway, pathways in cancer, and focal adhesion were overlapped

(Figure 7A-C). A total of 5 genes (BCL2, COL4A4, IGF1, LAMA4, and PDGFRA) were obtained, and these genes were considered hub targets (Figure 7D). A comprehensive meta-analysis was achieved by integrating 20 chip data and 1 sequencing data to assess the expression of these hub genes in HCC. The results indicate that only the LAMA4 gene was obviously upregulated in 1616 HCC tissues compared with 901 normal tissues (SMD = 1.18; 95% CI, 0.98 to 1.38; $P < 0.0001$) with

Table 5. GO and KEGG Pathway Analysis.

Category	Count	P-Value
Biological Process		
Signal transduction	68	2.39E-10
Peptidyl-tyrosine phosphorylation	19	7.42E-08
Activation of MAPK activity	15	5.71E-07
Angiogenesis	20	4.79E-06
Positive regulation of angiogenesis	14	7.57E-06
Cell Component		
Plasma membrane	169	3.48E-13
Integral component of plasma membrane	79	8.66E-12
Extracellular region	69	6.40E-06
Extracellular space	60	9.58E-06
Receptor complex	14	1.47E-05
Molecular Function		
Transmembrane receptor protein tyrosine kinase activity	10	3.31E-07
Ras guanyl-nucleotide exchange factor activity	15	1.23E-06
Protein tyrosine kinase activity	15	7.02E-06
Protein homodimerization activity	37	1.08E-04
Phosphatidylinositol-4,5-bisphosphate 3-kinase activity	9	1.60E-04
KEGG pathways		
Hsa04380: Osteoclast differentiation	15	1.53E-04
Hsa04060: Cytokine-cytokine receptor interaction	21	2.48E-04
Hsa04151: PI3K-Akt signaling pathway	26	3.14E-04
Hsa04610: Complement and coagulation cascades	10	5.48E-04
Hsa05200: Pathways in cancer	27	9.54E-04
Hsa05202: Transcriptional misregulation in cancer	15	0.001783834
Hsa04510: Focal adhesion	16	0.004845946
Hsa04015: Rap1 signaling pathway	16	0.00577715
Hsa04010: MAPK signaling pathway	18	0.006149439
Hsa04750: Inflammatory mediator regulation of TRP channels	10	0.00641923

heterogeneity using the random effects model ($P < 0.001$, $I^2 = 70.7\%$) (Table 6, Figure 8A). The protein expression of LAMA4 was assessed based on the immunohistochemistry data obtained from The Human Protein Atlas. The results indicate that LAMA4 was medium positive in HCC tissues and was negative in normal tissues (Figure 8B). In addition, the sROC curve indicates that LAMA4 has the potential to differentiate HCC tissues from normal tissues, with the AUC being 0.86. The corresponding sensitivity and specificity were 0.92 (0.86, 0.95) and 0.71 (0.64, 0.78), respectively (Table 7, Figure 8C, Supplementary Figure 2). The prognosis value of LAMA4 was determined in our prognosis meta-analysis, with the HR being 2.64 (2.06, 3.36).

Transcription Factors and the miR-199a-3p Co-Regulatory Network

A total of 15 TF-miR-199a-3p regulatory axes were identified in CMTCN, which included 11 co-regulatory pairs, 3 TF-FFLs, and 2 composite-FFLs (Table 8). The transcription factor and the miR-199a-3p co-regulatory network were constructed with Cytoscape 5.3.0 (Figure 9). In the network, several hub genes

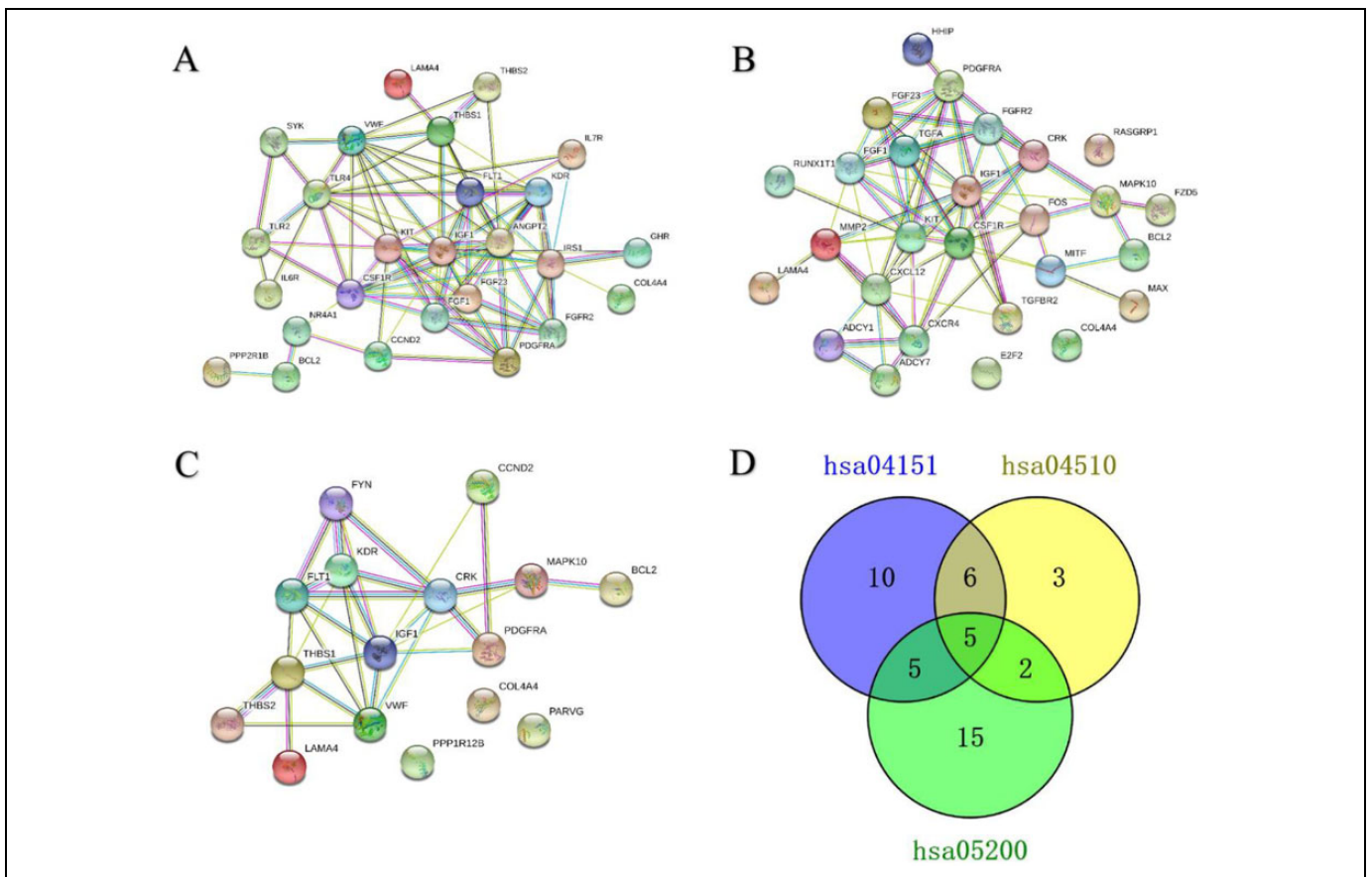


Figure 7. Identification of the hub target genes of miR-199a-3p in HCC. A: the PPI network based on the gene enriched in PI3K-Akt signaling pathway; B: the PPI network based on the gene enriched in pathways in cancer; C: the PPI network based on the gene enriched in focal adhesion; D: the hub target genes of miR-199a-3p.

Table 6. The Evaluation of LAMA4 Expression in HCC Based on HCC Chip Data and Sequencing Data.

ID	Number	Mean	SD	Number	Mean	SD	T	P-Value
GSE112790	183	6.2766	0.94726	15	4.953	0.50741	-5.34	P < 0.001
GSE121248	70	7.4552	0.78588	37	6.9014	0.48156	-4.508	P < 0.001
GSE84005	38	7.7395	0.77182	38	6.5824	0.42431	-8.098	P < 0.001
GSE84402	14	5.6971	1.13629	14	5.0262	0.43444	-2.064	0.055
GSE45050	6	8.4942	1.78201	3	6.9468	0.19627	-1.45	0.19
GSE107170	119	7.3565	1.05779	159	6.784	0.6781	-5.164	P < 0.001
GSE102079	152	6.1809	0.98857	105	5.2455	0.60178	-9.412	P < 0.001
GSE12941	10	7.2481	0.64296	10	6.1593	0.28869	-4.885	P < 0.001
GSE62232	81	6.221	1.0005	10	4.9682	0.44333	-7.002	P < 0.001
GSE60502	18	8.0719	0.67196	18	7.311	0.45714	-3.972	P < 0.001
GSE64041	60	7.857	0.68353	65	6.867	0.67969	-8.114	P < 0.001
GSE45436	93	6.0818	0.86424	41	4.9282	0.57197	-9.116	P < 0.001
GSE22405	24	5.169	0.18725	24	5.1841	0.13047	0.325	0.747
GSE41804	20	9.1577	0.89139	20	8.4139	0.57338	-3.139	0.003
GSE29721	10	6.5134	1.02392	10	5.3157	0.71027	-3.039	0.007
GSE14520(GPL571)	22	5.0207	0.74798	21	4.1329	0.22024	-5.331	P < 0.001
GSE14520(GPL3921)	225	4.8977	0.8156	220	4.2834	0.47889	-9.715	P < 0.001
GSE19665	10	6.57	0.47982	10	6.1798	0.31741	-2.145	0.046
GSE6764	35	5.9652	1.02718	10	4.6917	0.63283	-3.707	0.001
GSE14323	55	5.7118	0.56923	19	4.8648	0.65386	-5.381	P < 0.001
TCGA	371	9.1875	0.97075	52	7.6927	0.73992	-10.674	P < 0.001

were found, including GATA2, SP1, SOD1, and PTGS2. Further verification was still needed.

Discussion

In this study, downregulated miR-199a-3p was identified in 1190 HCC tissues compared with 663 normal human tissues based on HCC chip data and sequencing data and qRT-PCR. MiR-199a-3p may serve as a biomarker for identifying HCC tissues and normal tissues. Additionally, we discovered a new potential target for miR-199a-3p that was associated with the regulation of key biological processes in HCC through enrichment analysis. Furthermore, a transcription factor and a miRNA regulatory network were constructed to further clarify the molecular mechanism of miR-199a-3p in HCC.

Downregulated miR-199a-3p can be observed in multiple cancers, such as esophageal cancer,¹⁶ papillary thyroid carcinoma,¹⁸ melanoma,²⁶ glioma,²⁷ testicular germ cell tumor,²⁸ prostate cancer stem cells,²⁹ renal cell carcinoma,³⁰ and osteosarcoma.^{31,32}

Many studies have documented the potential for clinical applications of miR-199a-3p in multiple cancers. The diagnostic value of serum miR-199a-3p has been concerned with lung cancer^{33,34} and glioma.³⁵ In addition, the prognostic value of miR-199a-3p has been reported in bladder cancer,³⁶ ovarian cancer,³⁷ and testicular tumor.³⁸ Moreover, miR-199a-3p may serve as a therapeutic target in pancreatic cancer,³⁹ testicular tumor,³⁸ and renal cell carcinoma.³⁰ Furthermore, miR-199a-3p reduced drug resistance or improved chemotherapy sensitivity in ovarian cancer,^{40,37} breast cancer,^{41,42} osteosarcoma,⁴³ and cholangiocarcinoma.⁴⁴

In HCC, it has been shown that miR-199a-3p can act on multiple targets to inhibit the growth, migration, invasion, and angiogenesis of HCC cells. For example, the latest study reports that abnormal expression of miR-199a-3p in liver cancer can target CDK7 and TACC2 and contribute to the occurrence and development of liver cancer.⁴⁵ Another study identified the potential feasibility of miR-199a-3p in the diagnosis and treatment of liver cancer by detecting the expression of miRNA in 18 pairs of HCC and matched non-tumor tissues.¹⁹ A study based on mouse liver cancer models showed that miR-199a-3p could inhibit the growth of liver cancer by regulating MTOR and PAK4 pathways.²¹ It has also been noted that miR-199a-3p can target E-cadherin and Notch1,²⁰ thus providing a new strategy for the treatment of liver cancer. In addition, some studies have shown that PUMA or ZHX1,²² VEGFA, VEGFR1, VEGFR2, HGF and MMP2,²³ YAP1, Jagged1 and Notch signals,²⁴ and CD151²⁵ may be the target genes of miR-199a-3p.

In short, the abnormal expression of miR-199a-3p in a variety of human malignant tumors may be an important molecular target for the clinical diagnosis and treatment of tumors, especially in HCC. However, the existing studies have only used small samples or a single experiment to evaluate the expression of miR-199a-3p in hepatocellular carcinoma, which greatly reduces the reliability of the conclusions. Moreover, the relevant molecular mechanisms have not yet been clarified. Our study combined a large number of samples and qRT-PCR data from multiple databases, and it further confirmed that miR-199a-3p is underexpressed in HCC. Additionally, the targets of miR-199a-3p were confirmed by integrating upregulated differentially expressed genes of HCC from multiple platforms, downregulated genes from miR-

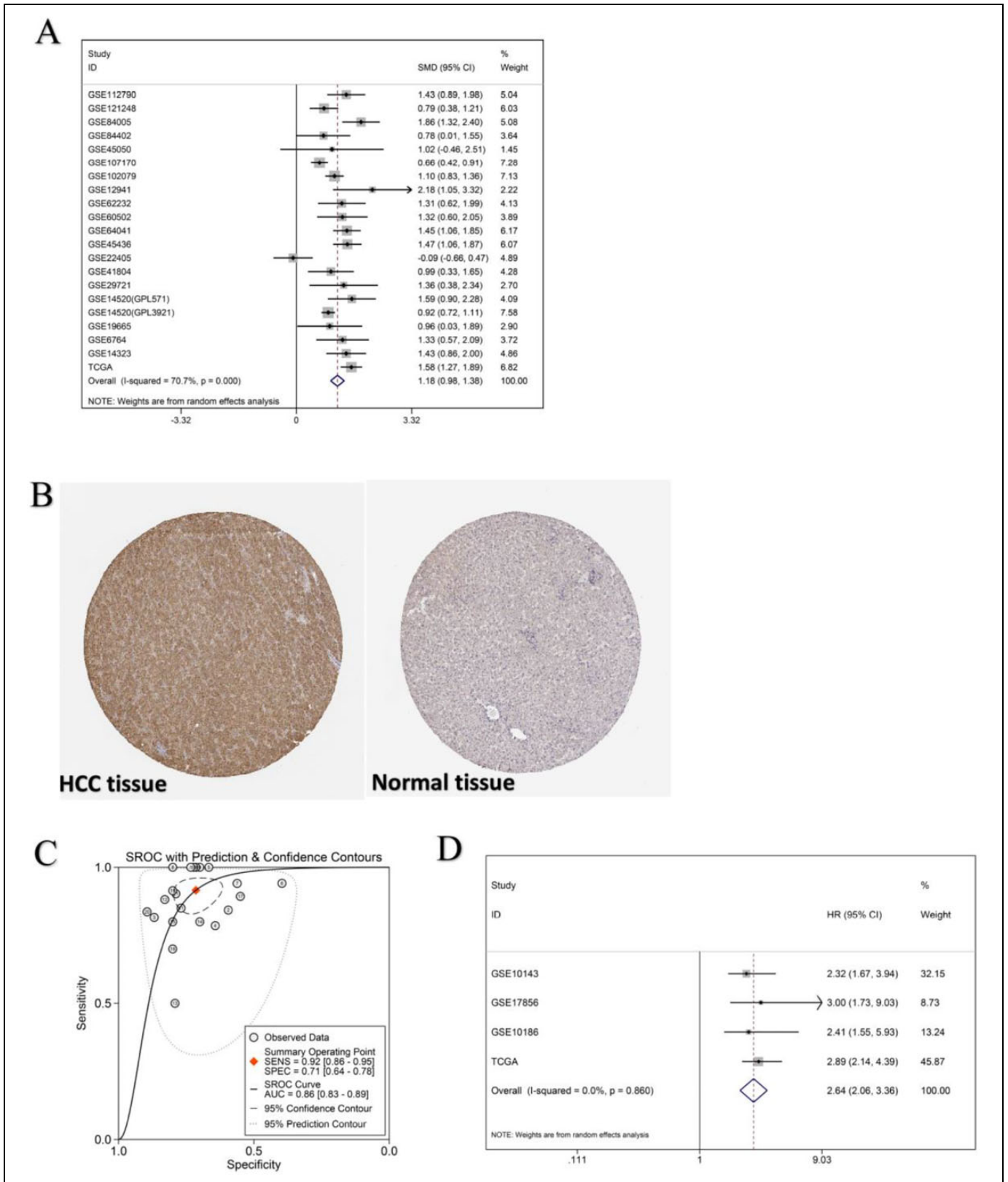


Figure 8. Validation of the hub target gene of miR-199a-3p. A: the evaluation of LAMA4 expression in HCC based on HCC chip data and sequencing data; B: the protein expression level of LAMA4 in HCC based on The Human Protein Atlas; C: SROC to assess the potential of LAMA4 in differentiating HCC tissues from normal tissues; D: prognosis-related meta-analysis to assess the prognostic value of LAMA4 based on multiple data sets.

199a-3p overexpressed and untreated HCC cell lines, and predicted targets of miR-199a-3p. This should greatly improve the accuracy of the target genes. Furthermore, we found that these target genes were mainly enriched in the PI3K-Akt signaling pathway, pathways in cancer, and focal adhesion. These pathways have been documented as being

closely related to the growth, migration, and invasion of multiple cancers, including HCC.

A recent study reported that upregulation of CFHR3 inhibited proliferation and increased apoptosis of HCC cells by suppressing the PI3K/Akt/mTOR signaling pathway.⁴⁶ The inhibition of SOCS5 can induce autophagy and reduce migration in HCC cells via the PI3K/Akt/mTOR pathway.⁴⁷ Anemomide B4 induces apoptosis of cancer cells by inhibiting the PI3K/Akt/mTOR pathway in HCC.⁴⁸ Pathways in cancer is a cancer-related pathway and has been reported to be a key pathway in multiple cancers, such as colorectal cancer⁴⁹ and thyroid cancer.⁵⁰ He *et al.* reported that overexpression of RBAK in lung cancer may increase cell migration and invasion via focal adhesion.⁵¹ Lu *et al.* discovered through integrative analysis that focal adhesion is a pathway in pancreatic cancer.⁵² Lou *et al.* indicated that focal adhesion is an HCC-related pathway and is closely involved in the invasion and metastasis of HCC.⁵³

According to the prediction of the online database, the 3'UTR of LAMA4 can be combined by miR-199a-3p. Additionally, the miR-199a-3p and LAMA4 expression data from the same patients of TCGA showed that miR-199a-3p was significantly lower in HCC, while LAMA4 was significantly higher in HCC. We identified LAMA4 as a potential target of miR-199a-3p in HCC in this study. So far, several studies have reported the important role of LAMA4 in multiple cancers. Li *et al.* verified that miR-200b was suppressed tumor metastasis in renal cell carcinoma by directly reducing LAMA4 expression.⁵⁴ A study by Wang *et al.* indicated that highly expressed LAMA4 was an independent, prognosis-related biomarker in gastric cancer.⁵⁵ Yang *et al.* suggested that LAMA4 plays a

Table 7. The Potential of LAMA4 in Identifying HCC Tissues From Normal Tissues.

ID	Sensitivity	Specificity	TP	FP	FN	TN
GSE112790	1	0.7596	183	4	0	11
GSE121248	0.8378	0.5857	59	15	11	22
GSE84005	0.8158	0.8684	31	5	7	33
GSE84402	0.7857	0.6429	11	5	3	9
GSE45050	1	0.8333	6	1	0	2
GSE107170	0.9434	0.395	112	96	7	63
GSE102079	0.9429	0.5658	143	46	9	59
GSE12941	1	0.8	10	2	0	8
GSE62232	1	0.7284	81	3	0	7
GSE60502	1	0.7222	18	5	0	13
GSE64041	0.8462	0.7667	51	15	9	50
GSE45436	0.878	0.828	82	7	11	34
GSE22405	0.5	0.7917	12	5	12	19
GSE41804	0.8	0.7	16	6	4	14
GSE29721	0.8	0.8	8	2	2	8
GSE14520(GPL571)	1	0.7273	22	6	0	15
GSE14520(GPL3921)	0.8955	0.5511	201	99	24	121
GSE19665	0.7	0.8	7	2	3	8
GSE6764	0.9	0.7714	32	2	3	8
GSE14323	0.8421	0.9091	46	2	9	17
TCGA	0.9038	0.7817	335	11	36	41

TP: true positive; FP: false positive; FN: false negative; TN: true negative.

Table 8. The Regulatory Network Between Transcription Factor and miR-199a-3p in HCC.

Genes	miRNAs	TFs	P_TG	P_TM	P_MG	R_TG	R_TM	R_MG
Co-regulated pairs								
SOD1	hsa-mir-199a-1	NFE2L2	0		0	-0.23267		-0.25387
SOD1	hsa-mir-199a-1	JUN	0		0	-0.24935		-0.25387
MAPK1	hsa-mir-199a-1	ASH1L	0.00004		0.00001	-0.20014		-0.21382
SOD1	hsa-mir-199a-1	PPARD	0		0	0.25875		-0.2825
SOD1	hsa-mir-199a-1	POLR2I	0		0	0.27164		-0.25387
SOD1	hsa-mir-199a-1	CEBPD	0		0	0.27164		-0.2825
PTGS2	hsa-mir-199a-1	APC	0		0	-0.48261		-0.27395
PTGS2	hsa-mir-199a-1	CTNNB1	0		0	0.60307		-0.27395
CNOT1	hsa-mir-199a-1	SMARCC1	0		0	-0.24219		-0.28161
PTGS2	hsa-mir-199a-1	NR0B2	0		0	0.3944		-0.27395
UBR5	hsa-mir-199a-1	ARID1B	0		0.00001	0.29831		-0.21992
TF feed-forward loops								
MAPK1	hsa-mir-199a-1	TP53	0	0	0.00001	0.4444	-0.2532	-0.21382
PTGS2	hsa-mir-199a-1	CEBPA	0	0	0	0.54698	-0.42045	-0.27395
ARHGAP35	hsa-mir-199a-1	ESR1	0	0.00002	0.00001	0.31633	-0.20653	-0.21445
Composite feed-forward loops								
CNOT1	hsa-mir-199a-1	GATA2	0	0	0	0.4792	-0.31303	-0.28161
SOD1	hsa-mir-199a-1	SP1	0	0.00003	0	0.45558	-0.20106	-0.2825

The P_TG, P_TM, and P_MG represent the Spearman's correlation p-value between TF, TF-miRNA, and miRNA gene expression, respectively. The R_TG, R_TM, and R_MG represent the Spearman's correlation coefficient between TF, TF-miRNA, and miRNA gene expression, respectively.

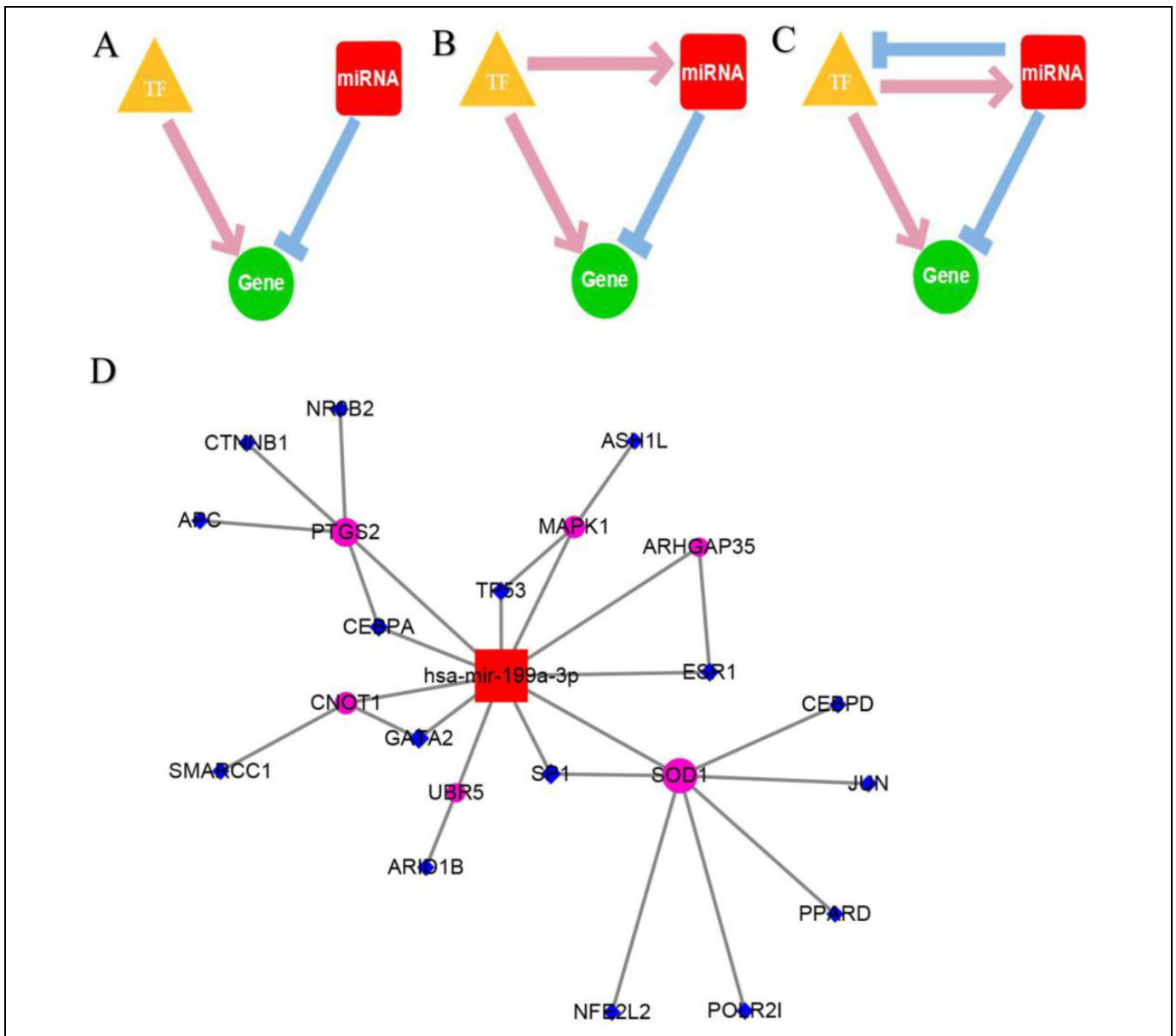


Figure 9. Construction of the transcription factor and miR-199a-3p regulatory network. A: the model of co-regulatory pairs; B: the model of TF-FFLs; C: the model of composite-FFLs; D: the regulatory network of transcription and miR-199a-3p.

vital role in tumor evolution and may be a key target in the treatment of triple-negative breast cancer.⁵⁶ Regarding HCC, Huang *et al.* reported that highly expressed LAMA4 in human HCC was identified in Chinese patients and has a strong correlation with tumor invasion and metastasis.⁵⁷ **Further *in vivo* and *in vitro* verification are still needed.**

Conclusion

In summary, the target of miR-199a-3p was involved in some important cancer-related pathways, and the hub target gene, LAMA4, has been reported to be closely associated with

invasion and metastasis of HCC. Therefore, we conclude that down-miR-199a-3p is a crucial tumor suppressor in HCC.

Author Contributions

An-gui Liu, B.Med., Yu-yan Pang, M.D Contributed equally.

Acknowledgments

The authors would like to thank all members of the Molecular Oncology Group of the First Affiliated Hospital of Guangxi Medical University (Nanning, Guangxi Zhuang Autonomous Region 530021, China) for their professional suggestions. At the same time, thanks

to GEO, SRA, TCGA, Human Protein Atlas and other websites for providing valuable data.

Ethics Approval and Consent to Participate

This research programme was approved by the Ethics Committee of The First Affiliated Hospital of Guangxi Medical University (2019-KY-NSFC-101, 2019-KY-NSFC-113). All participants signed informed consent forms.

Declaration of Conflicting Interests

The author(s) declared no potential conflicts of interest with respect to the research, authorship, and/or publication of this article.

Funding

The author(s) disclosed receipt of the following financial support for the research, authorship, and/or publication of this article: The study was supported partly by the Funds of Natural Science Foundation of Guangxi, China (2018JJA140409, 2017GXNSFAA198026, 2015GXNSFBA139157), Youth Science Foundation of Guangxi Medical University (GXMUYSF201624), Guangxi Degree and Post-graduate Education Reform and Development Research Projects, China (JGY2019050), 2019 Guangxi Medical University Education and Teaching Reform Project (2019XJGZ04), Future Academic Star of Guangxi Medical University (WLXSZX19077). Project of Science and Technology Innovation Training Program of the First Clinical Medical College of Guangxi Medical University(2018YFYB08).

ORCID iD

Jie Ma  <https://orcid.org/0000-0001-5545-2651>

Supplemental Material

Supplemental material for this article is available online.

References

- Siegel RL, Miller KD, Jemal A. Cancer statistics, 2019. *CA Cancer J Clin.* 2019;69(1):7-34.
- Espelt MV, Bacigalupo ML, Carabias P, Troncoso MF. MicroRNAs contribute to ATP-binding cassette transporter- and autophagy-mediated chemoresistance in hepatocellular carcinoma. *World J Hepatol.* 2019;11(4):344-358.
- Wang L, Wang FS. Clinical immunology and immunotherapy for hepatocellular carcinoma: current progress and challenges. *Hepatology Int.* 2019;13(5):521-533.
- Miller KD, Nogueira L, Mariotto AB, et al. Cancer treatment and survivorship statistics, 2019. *CA Cancer J Clin.* 2019;69(5):363-385.
- Qiu H, Zhang G, Song B, Jia J. MicroRNA-548b inhibits proliferation and invasion of hepatocellular carcinoma cells by directly targeting specificity protein 1. *Exp Ther Med.* 2019;18(3):2332-2340.
- Rawat M, Kadian K, Gupta Y, et al. MicroRNA in pancreatic cancer: from biology to therapeutic potential. *Genes (Basel).* 2019;10(10):752.
- Wang S, Claret FX, Wu W. MicroRNAs as therapeutic targets in nasopharyngeal carcinoma. *Front Oncol.* 2019;9:756.
- Jia X, Wang X, Guo X, et al. MicroRNA-124: an emerging therapeutic target in cancer. *Cancer Med.* 2019;8(12):5638-5650.
- Moody L, Dvoretzkiy S, An R, Mantha S, Pan YX. The efficacy of miR-20a as a diagnostic and prognostic biomarker for colorectal cancer: a systematic review and meta-analysis. *Cancers (Basel).* 2019;11(8):111.
- Zhang L, Li B, Zhang B, Zhang H, Suo J. miR-361 enhances sensitivity to 5-fluorouracil by targeting the FOXM1-ABCC5/10 signaling pathway in colorectal cancer. *Oncol Lett.* 2019;18(4):4064-4073.
- Naeli P, Yousefi F, Ghasemi Y, Savardashtaki A, Mirzaei H. The role of microRNAs in lung cancer: implications for diagnosis and therapy. *Curr Mol Med.* 2020;20(2):90-101.
- Lu L, Wu M, Lu Y, et al. MicroRNA-424 regulates cisplatin resistance of gastric cancer by targeting SMURF1 based on GEO database and primary validation in human gastric cancer tissues. *Onco Targets Ther.* 2019;12:7623-7636.
- Lu Z, Li X, Xu Y, et al. microRNA-17 functions as an oncogene by downregulating Smad3 expression in hepatocellular carcinoma. *Cell Death Dis.* 2019;10(10):723.
- El Mahdy HA, Abdelhamid IA, Amen AI, Abdelsameea E, Hassouna MM. MicroRNA-215 as a diagnostic marker in Egyptian patients with hepatocellular carcinoma. *Asian Pac J Cancer Prev.* 2019;20(9):2723-2731.
- Qu J, Yang J, Chen M, et al. MicroRNA-21 as a diagnostic marker for hepatocellular carcinoma: a systematic review and meta-analysis. *Pak J Med Sci.* 2019;35(5):1466-1471.
- Phatak P, Burrows WM, Chesnick IE, et al. MiR-199a-3p decreases esophageal cancer cell proliferation by targeting p21 activated kinase 4. *Oncotarget.* 2018;9(47):28391-28407.
- Qu F, Zheng J, Gan W, et al. MiR-199a-3p suppresses proliferation and invasion of prostate cancer cells by targeting Smad1. *Oncotarget.* 2017;8(32):52465-52473.
- Liu C, Xing M, Wang L, Zhang K. miR-199a-3p downregulation in thyroid tissues is associated with invasion and metastasis of papillary thyroid carcinoma. *Br J Biomed Sci.* 2017;74(2):90-94.
- Zhu HR, Huang RZ, Yu XN, et al. Microarray expression profiling of microRNAs reveals potential biomarkers for hepatocellular carcinoma. *Tohoku J Exp Med.* 2018;245(2):89-98.
- Giovannini C, Fornari F, Dallo R, et al. MiR-199-3p replacement affects E-cadherin expression through Notch1 targeting in hepatocellular carcinoma. *Acta Histochem.* 2018;120(2):95-102.
- Callegari E, D'Abundo L, Guerriero P, et al. miR-199a-3p modulates MTOR and PAK4 pathways and inhibits tumor growth in a hepatocellular carcinoma transgenic mouse model. *Mol Ther Nucleic Acids.* 2018;11:485-493.
- Guan J, Liu Z, Xiao M, et al. MicroRNA-199a-3p inhibits tumorigenesis of hepatocellular carcinoma cells by targeting ZHX1/PUMA signal. *Am J Transl Res.* 2017;9(5):2457-2465.
- Ghosh A, Dasgupta D, Ghosh A, et al. MiRNA199a-3p suppresses tumor growth, migration, invasion and angiogenesis in hepatocellular carcinoma by targeting VEGFA, VEGFR1, VEGFR2, HGF and MMP2. *Cell Death Dis.* 2017;8(3):e2706.

24. Ren K, Li T, Zhang W, Ren J, Li Z, Wu G. miR-199a-3p inhibits cell proliferation and induces apoptosis by targeting YAP1, suppressing Jagged1-Notch signaling in human hepatocellular carcinoma. *J Biomed Sci.* 2016;23(1):79.
25. Kim JH, Badawi M, Park JK, et al. Anti-invasion and anti-migration effects of miR-199a-3p in hepatocellular carcinoma are due in part to targeting CD151. *Int J Oncol.* 2016;49(5):2037-2045.
26. Liang L, Zhang Z, Qin X, et al. Gambogic acid inhibits melanoma through regulation of miR-199a-3p/ZEB1 signalling. *Basic Clin Pharmacol Toxicol.* 2018;123(6):692-703.
27. Shen L, Sun C, Li Y, et al. MicroRNA-199a-3p suppresses glioma cell proliferation by regulating the AKT/mTOR signaling pathway. *Tumour Biol.* 2015;36(9):6929-6938.
28. Chen BF, Gu S, Suen YK, Li L, Chan WY. microRNA-199a-3p, DNMT3A, and aberrant DNA methylation in testicular cancer. *Epigenetics.* 2014;9(1):119-128.
29. Liu R, Liu C, Zhang D, et al. miR-199a-3p targets stemness-related and mitogenic signaling pathways to suppress the expansion and tumorigenic capabilities of prostate cancer stem cells. *Oncotarget.* 2016;7(35):56628-56642.
30. Liu J, Liu B, Guo Y, et al. MiR-199a-3p acts as a tumor suppressor in clear cell renal cell carcinoma. *Pathol Res Pract.* 2018;214(6):806-813.
31. Gao Y, Feng Y, Shen JK, et al. CD44 is a direct target of miR-199a-3p and contributes to aggressive progression in osteosarcoma. *Sci Rep.* 2015;5:11365.
32. Duan Z, Choy E, Harmon D, et al. MicroRNA-199a-3p is downregulated in human osteosarcoma and regulates cell proliferation and migration. *Mol Cancer Ther.* 2011;10(8):1337-1345.
33. He Y, Ren S, Wang Y, Li X, Zhou C, Hirsch FR. Serum microRNAs improving the diagnostic accuracy in lung cancer presenting with pulmonary nodules. *J Thorac Dis.* 2018;10(8):5080-5085.
34. Zhu Y, Li T, Chen G, et al. Identification of a serum microRNA expression signature for detection of lung cancer, involving miR-23b, miR-221, miR-148b and miR-423-3p. *Lung Cancer.* 2017;114:6-11.
35. Chai C, Song LJ, Yang B, Han SY, Li XQ, Li M. Circulating miR-199a-3p in plasma and its potential diagnostic and prognostic value in glioma. *Eur Rev Med Pharmacol Sci.* 2016;20(23):4885-4890.
36. Sakaguchi T, Yoshino H, Yonemori M, et al. Regulation of ITGA3 by the dual-stranded microRNA-199 family as a potential prognostic marker in bladder cancer. *Br J Cancer.* 2017;116(8):1077-1087.
37. Petrillo M, Zannoni GF, Beltrame L, et al. Identification of high-grade serous ovarian cancer miRNA species associated with survival and drug response in patients receiving neoadjuvant chemotherapy: a retrospective longitudinal analysis using matched tumor biopsies. *Ann Oncol.* 2016;27(4):625-634.
38. Liu X, Duan H, Zhou S, et al. microRNA-199a-3p functions as tumor suppressor by regulating glucose metabolism in testicular germ cell tumors. *Mol Med Rep.* 2016;14(3):2311-2320.
39. Kuninty PR, Bojmar L, Tjomsland V, et al. MicroRNA-199a and -214 as potential therapeutic targets in pancreatic stellate cells in pancreatic tumor. *Oncotarget.* 2016;7(13):16396-16408.
40. Cui Y, Wu F, Tian D, et al. miR-199a-3p enhances cisplatin sensitivity of ovarian cancer cells by targeting ITGB8. *Oncol Rep.* 2018;39(4):1649-1657.
41. Freres P, Bouznad N, Servais L, et al. Variations of circulating cardiac biomarkers during and after anthracycline-containing chemotherapy in breast cancer patients. *BMC Cancer.* 2018;18(1):102.
42. Fan X, Zhou S, Zheng M, Deng X, Yi Y, Huang T. MiR-199a-3p enhances breast cancer cell sensitivity to cisplatin by downregulating TFAM (TFAM). *Biomed Pharmacother.* 2017;88:507-514.
43. Xu JF, Wang YP, Zhang SJ, et al. Exosomes containing differential expression of microRNA and mRNA in osteosarcoma that can predict response to chemotherapy. *Oncotarget.* 2017;8(44):75968-75978.
44. Li Q, Xia X, Ji J, et al. MiR-199a-3p enhances cisplatin sensitivity of cholangiocarcinoma cells by inhibiting mTOR signaling pathway and expression of MDR1. *Oncotarget.* 2017;8(20):33621-33630.
45. Wakasugi H, Takahashi H, Niinuma T, et al. Dysregulation of miRNA in chronic hepatitis B is associated with hepatocellular carcinoma risk after nucleos(t)ide analogue treatment. *Cancer Lett.* 2018;434:91-100.
46. Liu H, Zhang L, Wang P. Complement factor H-related 3 overexpression affects hepatocellular carcinoma proliferation and apoptosis. *Mol Med Rep.* 2019;20(3):2694-2702.
47. Zhang M, Liu S, Chua MS, et al. SOCS5 inhibition induces autophagy to impair metastasis in hepatocellular carcinoma cells via the PI3K/Akt/mTOR pathway. *Cell Death Dis.* 2019;10(8):612.
48. Xue S, Zhou Y, Zhang J, et al. Anemoside B4 exerts anti-cancer effect by inducing apoptosis and autophagy through inhibition of PI3K/Akt/mTOR pathway in hepatocellular carcinoma. *Am J Transl Res.* 2019;11(4):2580-2589.
49. Zhu H, Ji Y, Li W, Wu M. Identification of key pathways and genes in colorectal cancer to predict the prognosis based on mRNA interaction network. *Oncol Lett.* 2019;18(4):3778-3786.
50. Liang W, Sun F. Identification of pivotal lncRNAs in papillary thyroid cancer using lncRNA-mRNA-miRNA ceRNA network analysis. *PeerJ.* 2019;7:e7441.
51. He B, Wang B, Wang H, et al. RBAK is upregulated in non-small cell lung cancer and promotes cell migration and invasion. *Exp Ther Med.* 2019;18(4):2942-2948.
52. Lu W, Li N, Liao F. Identification of key genes and pathways in pancreatic cancer gene expression profile by integrative analysis. *Genes (Basel).* 2019;10(8):612.
53. Lou W, Chen J, Ding B, et al. Identification of invasion-metastasis-associated microRNAs in hepatocellular carcinoma based on bioinformatic analysis and experimental validation. *J Transl Med.* 2018;16(1):266.

54. Li Y, Guan B, Liu J, et al. MicroRNA-200b is downregulated and suppresses metastasis by targeting LAMA4 in renal cell carcinoma. *EBioMedicine*. 2019;44:439-451.
55. Wang X, Hou Q, Zhou X. LAMA4 expression is activated by zinc finger Eboxbinding homeobox 1 and independently predicts poor overall survival in gastric cancer. *Oncol Rep*. 2018;40(3):1725-1733.
56. Yang ZX, Zhang B, Wei J, et al. MiR-539 inhibits proliferation and migration of triple-negative breast cancer cells by down-regulating LAMA4 expression. *Cancer Cell Int*. 2018;18:16.
57. Huang X, Ji G, Wu Y, Wan B, Yu L. LAMA4, highly expressed in human hepatocellular carcinoma from Chinese patients, is a novel marker of tumor invasion and metastasis. *J Cancer Res Clin Oncol*. 2008;134(6):705-714.